Phospholipase A_2 Engineering. X-ray Structural and Functional Evidence for the Interaction of Lysine-56 with Substrates[†,‡]

Joseph P. Noel,[§,∥] Craig A. Bingman,[⊥] Tiliang Deng,[§,#] Cynthia M. Dupureur,[§] Kelly J. Hamilton,[§] Ru-Tai Jiang,[§] Jae-Gyu Kwak,[§] Chandra Sekharudu,[⊥] Muttaiya Sundaralingam,*[,⊥] and Ming-Daw Tsai*[,§]

Department of Chemistry and Ohio State Biotechnology Center, The Ohio State University, Columbus, Ohio 43210

Received May 17, 1991; Revised Manuscript Received August 8, 1991

ABSTRACT: Site-directed mutagenesis studies of bovine pancreatic phospholipase A_2 (PLA2, overproduced in *Escherichia coli*) showed that replacement of surface residue Lys-56 by a neutral or hydrophobic amino acid residue resulted in an unexpected and significant change in the function of the enzyme. The k_{cat} for phosphatidylcholine micelles increases 3–4-fold for K56M, K56I, and K56F and ca. 2-fold for K56N and K56T but does not change for K56R. These results suggest that the side chain of residue 56 has significant influence on the activity of PLA2. In order to probe the structural basis for the enhanced activity, the crystal structures of wild-type and K56M PLA2 were determined by X-ray crystallography to a resolution of 1.8 Å. The results suggest that the mutation has not only perturbed the conformation of the side chain of Met-56 locally but also caused conformational changes in the neighboring loop (residues 60–70), resulting in the formation of a hydrophobic pocket by residues Met-56, Tyr-52, and Tyr-69. Docking of a phosphatidylcholine inhibitor analogue into the active site of K56M, according to the structure of the complex of cobra venom PLA2–phosphatidylethanolamine inhibitor analogue [White, S. P., Scott, D. L., Otwinowski, Z., Gleb, M. H., & Sigler, P. (1990) *Science 250*, 1560–1563], showed that the choice moiety $[N(CH_3)_3]^+$ is readily accommodated into the newly formed hydrophobic pocket with a high degree of surface complementarity. This suggests a possible interaction between residue 56 and the head group of the phospholipid, explaining the enhanced activities observed when the positively charged Lys-56 is substituted by apolar residues, viz., K56M, K56I, and K56F. Further support for this interpretation comes from the 5-fold enhancement in k_{cat} for the mutant K56E with a negatively charged side chain, where there would be an attractive electrostatic interaction between the side chain of Glu-56 and the positively charged choline moiety. Our results also refute a recent report [Tomasselli, A. G., Hui, J., Fisher, J., Zürcher-Neely, H., Reardon, I. M., Oriaku, E., Kézdy, F. J., & Heinrikson, R. L. (1989) *J. Biol. Chem. 264*, 10041–10047] that substrate-level acylation of Lys-56 is an obligatory step in the catalysis by PLA2.

Despite extensive studies in many laboratories during the past two decades (Volwerk & de Haas, 1982; Dennis, 1983; Waite, 1987), the structure–function relationship of phospholipase A_2 (PLA2)[1] is a relatively underdeveloped subject. We therefore initiated structure–function studies using site-directed mutagenesis for PLA2 from bovine pancreas. The design, synthesis, and high-level expression (in *Escherichia coli*) of a gene for bovine pancreatic pro-PLA2 were initially reported by Noel and Tsai (1989). However, this expression system was very unstable and rendered large-scale preparation impossible. We then constructed an improved expression vector pTO (Deng et al., 1990) by combining the useful features of pIN-III-ompA3 (Ghrayeb et al., 1984) and pET-3a (Rosenberg et al., 1987) vectors. The level of expression in these systems appears to be higher than those reported recently for porcine (de Geus et al., 1987; Van den Bergh et al., 1987) and bovine (Tanaka et al., 1988) pancreatic PLA2.

The focus of this paper is to describe the refolding, purification, and characterization of WT PLA2 and mutant enzymes of Lys-56, a charged surface residue, and to rationalize the structure–function relationship. The choice of Lys-56 as the site of mutation was based on an interesting but puzzling report by Tomasselli et al. (1989) that porcine pancreatic PLA2 formed a highly activated (ca. 100-fold) dimer via substrate-level acylation of Lys-56. They demonstrated that the acylation was effected by a poor substrate analogue 4-nitro-3-(octanoyloxy)benzoic acid (NOB) as well as natural DPPC vesicles and further suggested that interfacial activation

[†] This work was supported by Research Grants GM41788 (to M.-D. T.) and GM18455 (to M.S.) from National Institutes of Health, and by a Monsanto fellowship to J.P.N. A preliminary account of part of the results has been published (Noel et al., 1990). This is paper 5 in the series entitled Phospholipase A_2 Engineering. For paper 4, see Dupureur et al. (1990).

[‡] The coordinates of WT and K56M PLA2 have been deposited at the Brookhaven Protein Data Bank.

[§] Department of Chemistry.

[∥] Current address: Department of Molecular Biophysics and Biochemistry, Yale University, New Haven, CT 06511.

[⊥] Department of Chemistry and Biotechnology Center.

[#] Current address: Department of Pharmacology, School of Medicine, University of California at San Diego, La Jolla, CA 92093.

[1] Abbreviations: CMC, critical micelle concentration; DC_6PC, 1,2-dihexanoyl-*sn*-glycero-3-phosphocholine; DC_7PC, 1,2-diheptanoyl-*sn*-glycero-3-phosphocholine; DC_8PC, 1,2-dioctanoyl-*sn*-glycero-3-phosphocholine; DPPC, 1,2-dipalmitoyl-*sn*-glycero-3-phosphocholine; $DC_{12}PG$, 1,2-dilauroyl-*sn*-glycero-3-phosphoglycerol; dCTPαS, 2′-deoxycytidine 5′-*O*-(1-thiotriphosphate); EDTA, ethylenediaminetetraacetate; Ellman's reagent, 5,5′-dithiobis(2-nitrobenzoic acid); FPLC, fast protein liquid chromatography; IPTG, isopropyl β-D-thiogalactopyranoside; NOB, 4-nitro-3-(octanoyloxy)benzoic acid; [^{14}C]NOB, 4-nitro-3-([1-^{14}C]octanoyloxy)benzoic acid; NTSB, 2-nitro-5-(sulfothio)-benzoate; PLA2, phospholipase A_2; PAGE, polyacrylamide gel electrophoresis; PMSF, phenylmethanesulfonyl fluoride; SDS, sodium dodecyl sulfate; TLC, thin-layer chromatography; TPCK, *N*-tosyl-L-phenylalanine chloromethyl ketone; Tris, 2-amino-2-(hydroxymethyl)-1,3-propanediol; WT, wild type.

0006-2960/91/0430-11801$02.50/0

of monomeric phospholipases is due to substrate-level autoacylation resulting in fully potentiated dimeric enzymes. The acylation also eliminated the latency phase observed when the porcine enzyme was assayed on monolayers.

Attempting to test the role of Lys-56 as suggested above, we substituted this residue with Met, Phe, Ile, Asn, Thr, Arg, and Glu. Since substrate-level acylation cannot occur in K56M, K56F, and K56I, one might predict that these mutant enzymes would have very low activities. However, it was found that these mutant enzymes showed significant increases in k_{cat} and decreases in K_m for phosphatidylcholine (PC) substrates. These and other functional properties of the mutant enzymes then allowed us to critically evaluate the interpretations of Tomasselli et al. (1989) and to discuss the mechanism of PLA2 catalysis. To probe the structural basis for the enhanced activity, we have determined the crystal structures of WT and K56M by X-ray crystallography at 1.8-Å resolution and docked a PC substrate into the active site of K56M.

Materials and Methods

Materials and Routine Procedures. NOB was synthesized from 3-hydroxy-4-nitrobenzoic acid and octanoyl chloride (both from Aldrich) as described by Cho et al. (1988). [^{14}C]NOB (0.1 mCi/mmol) was synthesized analogously except for the use of 1-[^{14}C]octanoate (ICN Biochemicals). NTSB was synthesized from Ellman's reagent (Aldrich) according to the procedure of Thannhauser et al. (1984). Oligonucleotides were obtained from the Biochemical Instrument Center at The Ohio State University. TPCK-treated trypsin was purchased from Sigma. Urea and sodium sulfite were obtained from Aldrich. IPTG (free of dioxan) was purchased from Research Organics (Cleveland, OH). All phospholipid substrates were purchased from Avanti Polar Lipids (Birmingham, AL). Purity was routinely checked by TLC on silica gel plates (methanol/chloroform/water 5:4:1 by volume), and further purification was never necessary. Other chemicals and biochemicals were of the highest quality available commercially.

Dialyses of proteins were carried out with Spectra/Por dialysis tubing, 6000–8000-MW cutoff, obtained from Spectrum Medical Institute (Los Angeles, CA) and treated according to the manufacturer's instructions. SDS–PAGE analysis of proteins employed the Phast System (Pharmacia-LKB) on 20% acrylamide gels. Staining was accomplished with a sensitive silver nitrate kit. The desalting gel Bio-Gel P-6DG was obtained from Bio-Rad. The fast flow Sepharose-S and -Q resins (cation and anion exchangers, respectively) used for FPLC columns were obtained from Pharmacia-LKB. FPLC experiments were performed on a Pharmacia-LKB FPLC system. Routine high-resolution gel filtration chromatography of PLA2 samples was carried out by FPLC on a Superose 12 K10/30 column (Pharmacia-LKB). The column was equilibrated in and eluted with a 25 mM sodium borate buffer, pH 8.0, containing 25 mM $CaCl_2$ and 100 mM NaCl, at a flow rate of 0.15 mL/min.

Construction of Mutants. Except for K56E, the pro-PLA2 gene from the pTO–propla2 plasmid (Deng et al., 1990) was used to construct the mutants; for K56E, the mature PLA2 gene from the pTO–A2M plasmid (Deng et al., 1990) was used. The genes were subcloned into M13mp18. Site-directed mutants were constructed according to the dCTPαS method of Eckstein (Taylor et al., 1985a,b) by using an Amersham mutagenesis kit. The mutant enzymes K56M, K56N, K56R, and K56T were obtained from a doubly degenerate oligonucleotide, AA CAA GCT AXX AAA CTT GAT A, where X is a mixture of A, T, G, and C. The oligonucleotides used for the construction of K56I, K56F, and K56E were A GCT ATC AAG TTT AAT AGC TTG TTT ATA GCA A, A GCT ATC AAG TTT AAA AGC TTG TTT ATA GCA A, and C AAG TTT TTC AGC TTG, respectively.

Purification of Enzymes. Crotalus atrox PLA2 was a generous gift from Paul Sigler. Porcine PLA2 was purified and activated as described previously (Nieuwenhuizen et al., 1974). The native PLA2 from bovine pancreas was purified and activated according to Dutilh et al. (1975). The recombinant WT and mutant PLA2s were isolated from the *E. coli* expression host, BL21(DE3)[pLysS], carrying the pTO–propla2 plasmid (pTO–A2M in the case of K56E) (Deng et al., 1990), as described below.

(*a*) *Cell Growth and Isolation of Insoluble Proteins.* Typically, 12 1-L cultures were grown in a broth containing 15 g/L bactotryptone, 25 g/L yeast extract, 0.25 g/L ampicillin, 0.02 g/L chloramphenicol, and 10 mM $MgSO_4$, pH 7.5. When A_{600} reached 1.2, more ampicillin was added to a final concentration of 0.5 g/L, which was followed by addition of IPTG (final concentration 0.05 mM) to induce PLA2 synthesis. After growth continued for 4 h, the bacterial cells were isolated by centrifugation at 9000*g* for 5 min. The yield was generally 3–5 g of cells/L of culture, and the cell pellets were stored at −20 °C. After thawing at room temperature, the pellet was then resuspended in 300 mL of 0.1 M Tris buffer, pH 8.0, containing 10 mM EDTA and 0.5% (v/v) Triton X-100. Sonication on a VibraCell sonicator (Sonics and Materials, Inc., Danbury, CT) operating at 600 W was carried out with stirring at room temperature for 60 s with pulsing and repeated until the solution was homogeneous. After addition of 0.1 mM PMSF, the solution was allowed to stir for 15 min at room temperature, and the inclusion body was isolated by centrifugation for 10 min at 12000*g* and at 4 °C. The pellet was resuspended in another 300 mL of the original lysis buffer and treated as before (beginning from the sonication step).

(*b*) *Solubilization of Insoluble Proteins by Sulfonation* (Thannhauser & Scheraga, 1985). The insoluble pellet from the original 12-L culture was resuspended in 100 mL of 8.0 M urea solution containing 0.3 M Na_2SO_3 by vigorous stirring and intermittent sonication (only enough to solubilize the pellet) at 600 W over a period of 30 min. A total of 20 mL of a 50 mM NTSB solution was then added to the stirring solution. Modification of the sulfonated proteins was complete after 5 min as judged by no further increase in A_{412}, but stirring was continued for 30 min. The mixture was then centrifuged for 30 min at 27000*g* to remove any remaining insoluble particles, and the supernatant was dialyzed against three changes of 9 L of deionized water. Dialysis was continued further for 4 h against 0.3% (v/v) acetic acid to precipitate the sulfonated protein. The precipitate was then collected by centrifugation at 12000*g* for 10 min followed by washing with 250 mL of water and recentrifugation. As shown in Figure 1 (lane 1), the inclusion body pellet consists mainly of PLA2 (the two bands correspond to pre-pro-PLA2 and pro-PLA2).

(*c*) *Refolding.* The procedure used for porcine PLA2 (de Geus et al., 1987) was adopted with some modifications. The pellet of sulfonated proteins was resuspended in 100 mL of 50 mM sodium borate buffer, pH 8.5, containing 5 mM EDTA, 4 mM reduced glutathione, 2 mM oxidized glutathione, and 8.0 M urea by stirring with brief sonication (2 × 60 s at 600 W). The pH was then readjusted to 8.5 with 2.0 M NaOH. The protein concentration of this solution was ca. 0.8 mg/mL since A_{280} was in the range of 0.9–1.1. The solution was then diluted to 400 mL over a period of 2 h with

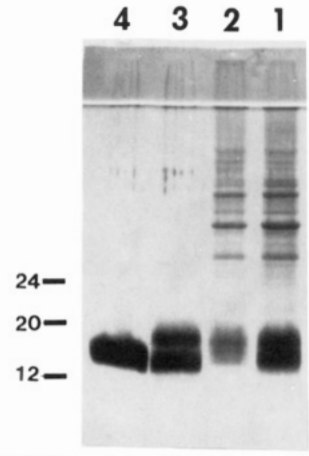

FIGURE 1: SDS–PAGE analysis of protein samples at different stages of the purification of WT PLA2: lane 1, insoluble inclusion pellet, before refolding; lane 2, insoluble pellet after refolding; lane 3, soluble fraction after refolding; lane 4, purified and activated PLA2. The additional strong band in lanes 1 and 3 is due to the pre-pro-PLA2.

300 mL of the same buffer without urea (the urea concentration of the final refolding solution was 2 M). The refolding was allowed to continue at room temperature for 10–12 h. The solution was then adjusted to pH 4.8 with glacial acetic acid and centrifuged at 12000*g* for 30 min at 4 °C. As shown by the SDS–PAGE analysis in Figure 1 (lanes 2 and 3), most *E. coli* proteins were removed during this step and the supernatant contained the refolded PLA2. Finally, the supernatant was concentrated to ca. 50 mL by placing it in dialysis tubing that was packed in dry sucrose for 12 h at 4 °C. The pH of the concentrate was adjusted to pH 7.8 and passed through a 600-mL Bio-Gel P-6DG column (5 cm × 30 cm) equilibrated in 50 mM NH_4HCO_3. The first peak eluting at the column void volume (ca. 75 mL) was lyophilized to yield 50–70 mg of crude pre-pro- and pro-PLA2.

(*d*) *Activation and Final Purification.* The lyophilized protein was dissolved in a 10 mM Tris buffer, pH 8.0 (25 °C), at a concentration of 5–10 mg/mL. TPCK-treated trypsin (Sigma) was then added to 0.2% (w/w PLA2), and the solution was stirred at room temperature. The pH was routinely monitored every 15 min and readjusted to 8.0 if necessary. The PLA2 activity was followed by a pH stat method (see next section) every 10–15 min. Once the activity reached a maximum (in ca. 100 min), PMSF was added to 0.1 mM to inactivate the trypsin. The solution was then diluted to 50 mL with deionized water, the pH was adjusted to 8.0, and the solution was applied to a 20-mL anion-exchange column (1.6 cm × 10 cm) of fast flow Sepharose-Q (preequilibrated in 10 mM Tris, pH 8.0, 25 °C) at a flow rate of 2 mL/min. The column was first washed with the equilibration buffer until A_{280} reached base line, then it was eluted with a 400-mL gradient (20 column bed volumes) from 0 to 0.25 M NaCl in the equilibration buffer at a flow rate of 2 mL/min. Active PLA2 typically eluted between 0.04 and 0.06 M NaCl. The PLA2-containing peak was pooled, dialyzed against 9 L of deionized water, adjusted to 10 mM sodium succinate, pH 4.5, and loaded on a 15-mL column (1.6 cm × 7.5 cm) of fast flow Sepharose-S. The column was first washed with 10 mM sodium succinate, pH 4.5, until A_{280} reached base line, then it was eluted with a 300-mL gradient from 0 to 0.4 M NaCl in 10 mM sodium succinate, pH 4.5. The PLA2 typically eluted between 0.12 and 0.14 M NaCl. The PLA2 peak was then buffer-exchanged on a Bio-Gel P-6DG column equilibrated in 50 mM NH_4HCO_3, pH 7.8. The protein peak was pooled and lyophilized, and the dry powder was stored at −20 °C. The SDS–PAGE profile of purified and activated PLA2 is shown in Figure 1 (lane 4). The PLA2 obtained above was either used directly or further purified by gel filtration on an FPLC Superose-12 column (1 cm × 30 cm) prior to kinetic analysis.

The purification of K56E was performed by a similar procedure except that the tryptic activation step was omitted since there was no pro-sequence. The refolded protein (before the P-6DG column) was applied directly to the fast flow Sepharose-S column, which separated the unprocessed pre-PLA2 from processed PLA2. The unprocessed pre-PLA2 was usually undetectable for WT PLA2, but it existed in significant amount (nearly 50%) for this mutant.

Assay and Kinetic Analysis of PLA2. (*a*) *Qualitative TLC Assays.* Routine assays used for following refolding and column profiles were carried out by TLC on silica gel plates. A small portion (5–10 μL) of a PLA2 solution was added to 30–50 μL of 10 mM Tris buffer, pH 8.0, containing 25 mM $CaCl_2$, 100 mM NaCl, 15 mM DC_8PC, and 0.1 μg of trypsin. After incubating for 5–10 min at room temperature, 1 μL of the assay mixture was spotted on a TLC plate next to a spot of unreacted DC_8PC. The plate was developed in 5:4:1 (v/v/v) methanol/chloroform/water and then stained with a phosphomolybdic acid solution in ethanol and heated. R_f vaules were 0.35 (DC_8PC) and 0.22 (lyso-DC_8PC).

(*b*) *Quantitative pH Stat Assays.* These assays were conducted at 45 °C with a Radiometer RTSS titration system. The reaction mixture consisted of a 2–4-mL solution containing 1 mM sodium borate, 25 mM $CaCl_2$, 100 mM NaCl, and the specified concentrations of substrate and/or detergent. After the reaction vessel was flushed with argon, the pH was adjusted to 8.0 with 10 mM NaOH, and PLA2 was added in a volume of 10–100 μL to start the reaction. The initial velocity was measured by recording the amount of 10 mM NaOH needed to maintain a constant pH of 8.0, usually observed within the first 3 min. The kinetic constants V_{max} and K_m were determined from Eadie–Hofstee plots (Atkins & Nimmo, 1975) of v vs $v/[S]$ by use of linear regression analyses. Errors in the calculated values were determined from such analyses. They are based upon the residuals measured from the actual data points and the theoretically determined linear line. The k_{cat} was calculated from V_{max} on the basis of the molecular weight of 13 500.

The PLA2 stock solution for kinetic analysis consists of 0.001–0.01 mg/mL PLA2 in the reaction buffer containing 5 mg/mL bovine plasma γ-globulin (Bio-Rad). A steady and reversible loss in activity was observed if the γ-globulin was absent. The precise concentration of PLA2 was determined by the A_{280} reading on the basis of $E_{0.1\%} = 1.3$ (Dutilh et al., 1975) prior to dilution into γ–globulin.

The ranges of substrate concentrations were 0.29–2.5 mM for monomeric DC_6PC, 0.10–0.71 mM for monomeric DC_7PC, 0.45–7.0 mM for micellar DC_7PC, and 0.28–5.0 mM for micellar DC_8PC. For micellar substrates, the concentrations of monomeric substrates at CMC have been subtracted from the total lipid concentration. In some cases duplicate or triplicate assays were performed at one concentration, and they agreed to within 5–10% of each other. This level of reproducibility is typical for lipolytic enzymes.

The negatively charged mixed micelles of $DC_{12}PG$ and sodium deoxycholate were prepared by mixing the former in chloroform and the latter in methanol at a mole ratio of 1:3, respectively. After thorough drying under vacuum, it was dissolved in a known volume of a 1 mM sodium borate/100 mM NaCl solution to give final concentrations of 5 mM

$DC_{12}PG$ and 15 mM deoxycholate. The solution was brought to 45 °C and pH 8.0 and incubated at this temperature until it became clear. Just before the kinetic run a 1.0 M $CaCl_2$ stock solution was added to give a final concentration of 5 mM $CaCl_2$. Since this substrate did not follow Michaelis–Menten kinetics, only specific activities were measured, and duplicate runs agreed to within 5% of each other.

(*c*) *Spectrophotometric Assays of NOB.* PLA2 was assayed against NOB at 37 °C in a thermostated cuvette in a Kontron Uvikon 930 spectrophotometer. The reaction mixture consisted of 1.0 mL of 25 mM Tris buffer, pH 8.0 (at 37 °C), containing 10 mM $CaCl_2$, 100 mM NaCl, and 7.75 μg of PLA2. The reaction was started by addition of microliter portions of a 13 mM solution of NOB in acetonitrile and monitored at A_{425} for the liberation of 4-nitro-3-hydroxybenzoate.

NOB Reactions. Experiments testing activation of PLA2 by NOB were carried out by incubating 0.25 mg of PLA2 with 0.31 mg of NOB in 1 mL of 25 mM Tris buffer, pH 8.0, containing 10 mM $CaCl_2$, 100 mM NaCl, and 1% (v/v) acetonitrile at 37 °C. Aliquots of 25 μL were removed at 1.5, 4.5, 10, 30, and 90 min and assayed against NOB as described above.

Acylations of porcine and bovine PLA2 by NOB were conducted as described by Tomasselli et al. (1989) except on a smaller scale (8 mg of enzyme, 50-fold molar excess of NOB, specific activity 0.1 mCi/mmol). After completion of the reaction, the solution was dialyzed extensively against deionized water, lyophilized, and desalted on a 10 mL Bio-Gel P-6DG desalting column equilibrated in 50 mM NH_4HCO_3. The protein fractions were pooled and lyophilized, and the desalting process was repeated until the yellow product of hydrolysis was totally removed and the specific radioactivity became constant.

X-ray Crystallographic Methods. Both WT and K56M were crystallized essentially as described previously for bovine pancreatic PLA2 (Dijkstra et al., 1978), in a 50 mM Tris buffer, pH 7.2, containing 5 mM $CaCl_2$ and 10–15 mg/mL lyophilized PLA2. It turns out that both WT and K56M gave trigonal crystals, space group $P3_121$, cell constants $a = b = 46.52$, $c = 102.20$ for WT and $a = b = 45.94$, $c = 102.487$ for K56M, in contrast to the orthorhombic crystals obtained previously (Dijkstra et al., 1978).

Intensity data on both crystals were collected on a Siemens area detector at Argonne National Laboratory out to resolutions of 1.65 Å for WT and 1.7 Å for K56M. The data were reduced using the XENGEN software package (Genex Corp, 1988; Gaithersburg, MD). There were 12 302 independent reflections [$F > 1\sigma(F)$] for WT with an $R_{sym}(F)$ of 4.11% and 11 523 independent reflections [$F > 1\sigma(F)$] for K56M with an $R_{sym}(F)$ of 4.53%. For this work the data out to a resolution of 1.8 Å were used since beyond 1.8 Å the mean $I/\sigma(I)$ drops below 3.

Although both WT and K56M crystals have the same space group and very similar cell constants compared to the crystals of bovine pro-PLA2 ($a = b = 46.95$, $c = 102.0$; Dijkstra et al., 1982), the latter was determined only at 3.0-Å resolution and showed considerable disorder. Therefore, we used the 1.7-Å structure of the orthorhombic form of bovine pancreatic PLA2 (Dijkstra et al., 1981a,b) as our starting model. The starting coordinates for our enzymes were obtained by superimposing the 1.7-Å orthorhombic form on the trigonal proenzyme. The resulting coordinates positioned in our cell gave an initial *R*-factor of 0.423 for WT for 2833 reflections between 5.0- and 2.5-Å resolution using all protein atoms excluding the calcium ion and water molecules. The X-PLOR program was used for the refinement. Initially, a rigid body refinement was carried out to accurately position the geometric center of the molecule. This procedure lowered the *R*-value to 0.362 with an overall *B* of 15 Å^2. The Sim-weighted difference electron density maps brought out the calcium ion as the most prominent peak (7 σ) at the expected location. The calcium ion was then included in subsequent refinements employing the simulated annealing protocol, which lowered the *R*-factor to 0.202 with an overall *B* of 12.7 Å^2 for the 2.5-Å resolution data. At this point the refinement was switched to the restrained least-squares method and a combination of omit map fitting while extending the data out to 1.8-Å resolution. The final *R*-factor was 18.8% for all the protein atoms, 85 water molecules, and a calcium ion for a total of 8925 reflections.

A similar procedure was used to refine the mutant K56M enzyme. The final *R*-factor was 18.6% at 1.8-Å resolution including 80 solvent molecules and a calcium ion for 8754 reflections. The R_{merge} between WT and K56M is 12.6%, which suggests that in addition to the Lys-56 to Met-56 substitution there are some significant local differences between WT and K56M. A difference electron density map computed using $|F_o(\text{K56M}) - F_o(\text{WT})|\alpha(\text{WT})$ as coefficients showed the highest positive peak (5 σ) at the position corresponding to the S^δ atom of Met-56, which confirmed the mutation of Lys-56. This map also contains a series of peaks near the loop (residues 60–70) explaining the relatively high value for R_{merge} between WT and K56M. The difference electron density maps of WT and K56M, omitting the residues 51–61, clearly showed the density for the side chains of Lys in WT and Met in K56M structures.

RESULTS

Purification and Characterization of Wild-Type and Mutant PLA2. With the exception of K56E, the enzymes in this work were produced in the form of pro-enzyme (along with some pre-pro-enzyme) with the pTO vector. Although the majority of the enzyme has been secreted into the periplasmic space and the pre-sequence has already been processed, the enzyme has not folded properly and is still largely insoluble, possibly due to the high cysteine content of this small enzyme (14 cysteine residues among a total of 123 amino acids) and the high concentration of the expressed protein in the periplasm. Thus, it was still necessary to solubilize and refold the enzyme. These and other purification procedures are described in detail in the experimental section. In brief, the purification procedure consists of the following major steps: (i) The inclusion body was isolated following cell breakage (sonication), detergent washing, and centrifugation. (ii) The insoluble inclusion body pellet was solubilized by sulfonation, first with sodium sulfite (which breaks a disulfide bridge into a free sulfhydryl group and a sulfonated sulfhydryl group) followed with NTSB (which sulfonates the free sulfhydryl group) (Thannhauser & Scheraga, 1985). (iii) The sulfonated protein was then subjected to refolding in the presence of urea and a glutathione redox couple (de Geus et al., 1987). (iv) The refolded protein was then activated by mild trypsinolysis and purified by anion-exchange and cation-exchange chromatography.

K56E was produced in the form of mature PLA2, and the trypsinolysis step was omitted. Kinetic and X-ray crystallographic analyses, as described in later sections, indicated that the recombinant WT PLA2 was identical to PLA2 isolated from its natural source, bovine pancreas.

It is important to note that the yield of the refolding step was not quantitative. Some improperly folded proteins always

Table I: Summary of Kinetic Data for Micellar Substrates[a]

enzyme	substrate	k_{cat} (s^{-1})	$K_{m,app}$ (mM)
bovine			
WT	DC_8PC	675	1.4
K56E	DC_8PC	2990	3.2
K56M	DC_8PC	2270	0.21
K56I	DC_8PC	2240	0.51
K56F	DC_8PC	2470	0.61
K56N	DC_8PC	1370	0.62
K56T	DC_8PC	1160	0.56
K56R	DC_8PC	510	0.75
bovine			
WT	DC_7PC	97	1.6
K56M	DC_7PC	420	0.35
bovine			
WT	$DC_{12}PG$	600	
K56E	$DC_{12}PG$	140	
K56M	$DC_{12}PG$	330	
K56N	$DC_{12}PG$	170	
K56T	$DC_{12}PG$	170	
porcine WT	DC_8PC[b]	410	3.2
porcine Δ62–66	DC_8PC[b]	980	1.9
C. atrox PLA2	DC_8PC	6350	0.18
C. adamanteus PLA2	DC_8PC[c]	4320	1.1

[a] The estimated errors for both k_{cat} and K_m are ±10% for PC substrates. The k_{cat} for $DC_{12}PG$ are turnover numbers at 5 mM substrate. [b] From Kuipers et al. (1989). Larger increases in activity (relative to WT) were observed with shorter chain substrates. [c] From Wells (1974).

formed but were separated by anion-exchange chromatography. Thus, it is possible that some of the mutant enzymes might fold differently and result in local or global conformational changes. This is a common problem for all site-specific mutant proteins, but disulfide mismatch is a particular concern for PLA2. It is therefore important to perform structural analysis when the chromatographic behavior of the mutant enzyme is different from that of the wild type and/or when the kinetic property of the mutant enzyme is significantly perturbed. This concern does not apply to the mutant enzymes described in this paper since they all behave similarly to the wild-type PLA2 chromatographically and their catalytic properties are enhanced, not impaired.

Lysine-56 Mutant Enzymes Show Enhanced Activity toward PC. There are many different ways to assay the activity of PLA2. DC_8PC was used as our standard micellar substrate for the kinetic studies of bovine pancreatic PLA2 and its mutant enzymes for the following reasons: the physiological substrates of pancreatic PLA2 are in micellar forms, PC is the most abundant phospholipid in nature, and PC with dioctanoyl chains (i.e., DC_8PC) appears to give the best activity with pancreatic PLA2 (Volwerk & de Haas, 1982). The shorter chain substrate DC_7PC was also used in some cases since with this substrate it is possible to compare micelles with monomers on the same substrate (the CMC of DC_8PC is too low to obtain good kinetic data for monomers). The k_{cat} and K_m values are summarized in Table I. The K_m for micelles are designated as $K_{m,app}$ since they reflect surface binding affinity instead of active site binding. As shown by the data in Table I, the K_{cat} of phosphatidylcholine micelles showed a ca. 5-fold increase for K56E, 3–4-fold increases for K56M, K56I, and K56F, ca. 2-fold increases for K56N and K56T, and no change for K56R. The $K_{m,app}$ values for some of the mutant enzymes also decreased by 2–7-fold, but our interpretation and discussion are mainly based on k_{cat} since the exact meaning of $K_{m,app}$ is not yet clear.

The kinetic constants of shorter chain DC_7PC and DC_6PC monomers have also been determined, and the data are listed in Table II. The results show increased k_{cat} and decreased K_m for K56M but not K56F or K56E. Since the activities of monomers are very low and the binding mode of monomers could be different from that of micelles, we have not further pursued monomeric studies.

The Activity for Negatively Charged Substrate Was Not Enhanced. A possible interpretation for the increased k_{cat} of the mutant enzymes toward DC_8PC micelles is that the side chain of residue 56 is involved in the interaction with the positively charged quaternary ammonium group of the choline chain. For positively charged residues such as lysine or arginine, the interaction is not favorable. For neutral residues the unfavorable interaction is relieved, and for negatively charged residues (in K56E) the interaction is enhanced. This interpretation would predict that the mutant enzymes should not show enhanced activity (or should show decreased activity) toward negatively charged substrates. To test this prediction, we examined the activity of WT and mutant PLA2s on negatively charged $DC_{12}PG$ (in the form of mixed micelles with deoxycholate). As shown in Table I, there was no enhancement in any case, and the activities, particularly that of K56E, actually decreased.

Structural Comparison of WT and K56M PLA2. We have solved the crystal structures of both WT and K56M at 1.8-Å resolution for two purposes: to quantify the effects of a single substitution on the structure of PLA2 and to understand the structural basis for the enhanced activity of K56M (and other mutants). Although the crystal structure of bovine pancreatic PLA2 had already been determined (Dijkstra et al., 1978) and refined to 1.7-Å resolution (Dijkstra et al., 1981a,b), we repeated the experiment as a means to unequivocally demonstrate that the genetically constructed enzyme is identical to the natural pancreatic enzyme. Surprisingly, our WT PLA2 formed trigonal crystals under conditions in which the pancreatic PLA2 formed orthorhombic crystals (except that there might be some residual NH_4HCO_3 in our proteins). Since K56M also formed trigonal crystals, the structures of WT and K56M can be compared using the same crystal forms.

The C_α atoms of our trigonal WT and K56M PLA2 show an overall rms deviation of 0.68 and 0.60 Å, respectively, with the orthorhombic PLA2 from bovine pancreas. These rms deviations are most likely caused by different crystal packing. Figure 2A shows the superposition of the C_α atoms of the trigonal WT and the orthorhombic WT, which indicate that the main regions of differences between the two structures are the loop 60–70 and the region near the calcium binding loop (residues 18–20 and 29–32). The superposition of the C_α atoms of WT and K56M as shown in Figure 2B gave a substantially lower rms (0.34 Å), which suggests very similar overall conformations. Since both WT and K56M have the same crystal forms, the subtle differences in their structures can be delineated and interpreted even though the overall backbone conformation of K56M is not significantly perturbed: (a) At the site of mutation the local backbone conformation has not been perturbed, but the side chain of residue 56 has undergone a major change in the $\chi 1$ angle, from gauche$^-$ in WT to gauche$^+$ in K56M (Figure 3). The remaining common side-chain dihedral angles $\chi 2$ and $\chi 3$ have similar values. (b) A change in the nature of the side chain has not only affected its conformation but also perturbed the conformation of the loop (residues 60–70) following the helix (residues 41–58) by drawing it closer as shown in Figure 2B. (c) In addition, the mutation has also significantly affected the ordering of the helix–loop segment. As shown in Figure 4, the WT structure shows significantly higher *B*-factors in the segment 55–70, compared to K56M. Possible explanations for these changes are discussed as follows.

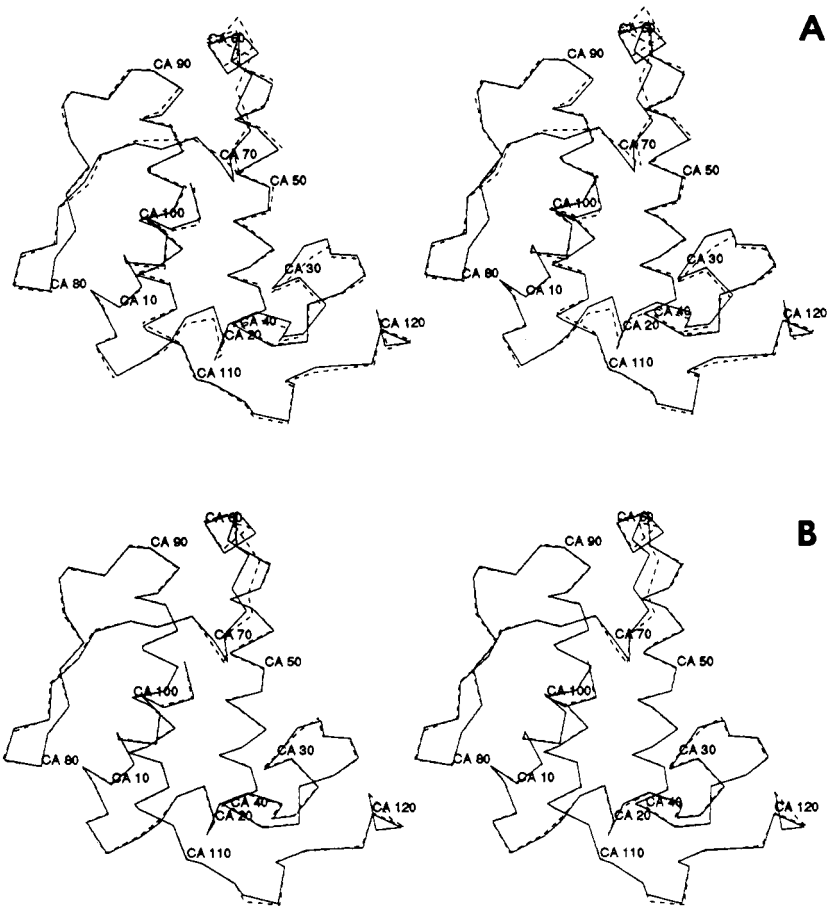

FIGURE 2: Stereoview of the α-carbon atom traces of bovine PLA2. (A) Superposition of the 1.8-Å trigonal PLA2 from this work (solid lines) and the 1.7-Å orthorhombic PLA2 from Dijkstra et al. (1981a,b) (dashed lines). (B) Superposition of the trigonal WT (solid lines) with the trigonal K56M (dashed lines) PLA2.

Substitution of Lys-56 by Met not only reduces the repulsive electrostatic interactions of the positively charged lysine triplet (Lys-53, Lys-56, and Lys-57) on the helix but also generates a new hydrophobic triplet (Tyr-52, Ala-55, and Met-56) which is known to enhance the stability of helices (Palau & Puigdomenech, 1974). This new hydrophobic triplet could draw Tyr-69 closer to it and enhance the aromatic–aromatic interaction (Burley & Petsko, 1985) between Tyr-69 and Tyr-52, leading to the formation of a hydrophobic pocket. These interactions could be responsible for the movement of the loop toward the helix as depicted in Figure 5, which could in turn result in the ordering of the helix–loop segment.

Docking of a Substrate into the Crystal Structure of K56M. To further understand the effects of mutation on substrate binding and catalysis, we have docked a molecule of DC_8PC into the active site of K56M according to the interactions reported by White et al. (1990) for the complex of *Naja naja atra* venom PLA2 with a transition-state analogue inhibitor. The binding mode in this complex is very similar to that of a related system with porcine pancreatic PLA2 (Thunnissen et al., 1990), but the inhibitor in neither complex contains a choline head group. The starting conformation of the phospholipid was conformation E in Table 7 of Sundaralingam (1972), and the *sn*-2 carbonyl group was made tetrahedral to mimic the transition state. With some conformational adjustments, the $N(CH_3)_3^+$ group fits well into the hydrophobic pocket formed by Met-56, Tyr-52, and Tyr-69, and is ca. 6 Å away from the ϵ-NH_3^+ of Lys-53 (Figure 6). For the WT PLA2, the same conformation will result in a repulsive electrostatic interaction between the $N(CH_3)_3^+$ group of the substrate analogue and the ϵ-NH_3^+ group of Lys-56. Thus, the K56M mutation could enhance the hydrophobic interactions between the choline head group and the enzyme. Comparison between Figure 6A and the Figure 3 of White et al. (1990) indicates that the conformations of the substrate analogues are very similar, except that the dihedral angle α_5 (O–C–C–N) of the head group is approximately −g for the former and +g for the latter. Both +g and −g conformations have been found in the crystal structure of $DC_{14}PC$ (Pearson & Pascher, 1979).

Lys-56 Acylation Is Not Part of the Catalytic Mechanism. The result that Lys-56 mutant enzymes showed at least a wild-type level of activities indicates that *acylation of Lys-56 could not be part of the catalytic mechanism of bovine pancreatic PLA2*, in contrast to the results and suggestion for the *porcine* enzyme by Tomasselli et al. (1989). There is, however, a possibility that the bovine and porcine enzymes could behave differently with regard to the effects of NOB. We therefore performed the following NOB experiments.

Using [^{14}C]NOB, we observed 34 and 23 mol % incorporation of the octanoyl group into bovine and porcine PLA2, respectively. The latter agreed well with the result of Tomasselli et al. (1989). As shown by the native PAGE gel in Figure 7, the NOB-treated bovine PLA2 (lane 4) showed one additional band relative to the untreated PLA2 (lane 3). The weak intensity of the additional band is consistent with the ^{14}C result that only ca. one-third of the enzyme is acylated. Although we did not isolate the acylated PLA2 and verify the site of acylation, the fact that no additional band resulted from treatment of K56M with NOB (lanes 1 and 2 in Figure 7) suggests that the acylation site of bovine PLA2 is indeed Lys-56 (same as porcine PLA2). Thus, we have confirmed

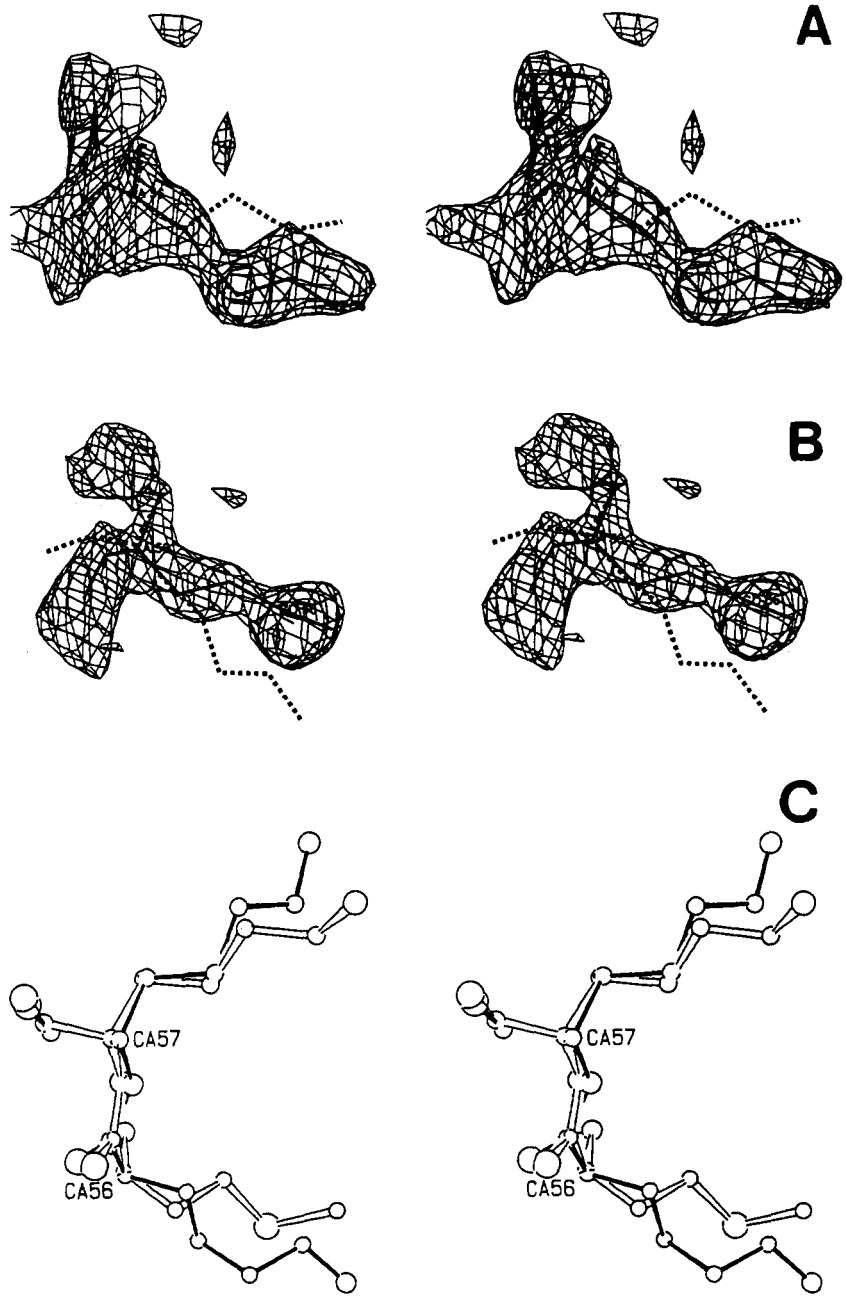

FIGURE 3: Stereoview showing the conformational differences between the side chains of residue 56 in WT and K56M. (A) The difference electron density (1.5 σ) for Lys-56, calculated using ($2F_o - F_c$) as Fourier coefficients with residues 51–60 omitted. The broken lines indicate the position for Met-56 in K56M. (B) The difference electron density showing Met-56 in the mutant enzyme. The broken lines indicate the position for Lys-56 in the WT. (C) The backbone atoms of residues 56 and 57 are superimposed (rms 0.23 Å) to show the changes in the side-chain conformations. It is noteworthy that Lys-56 and Lys-57 show a diverging conformation in WT (solid bonds) in contrast to Met-56 and Lys-57 in K56M (open bonds).

the acylation of *bovine* PLA2 by NOB, but the mutagenesis results suggest that acylation is not part of the catalytic mechanism. The same conclusion has been reached for the *porcine* PLA2 on the basis of different experiments by Jain et al. (1991a).

It is interesting to note that the NOB-modified bovine PLA2 runs at the same position as K56M in the native PAGE gel, as shown in Figure 7, possibly as a consequence of charge neutralization of residue 56 in both cases. Since Tomasselli et al. (1989) reported that the NOB-modified bovine PLA2 is a dimer, it may be asked whether K56M also dimerizes. As shown in Figure 8, the mutant enzyme K56M is clearly a monomer on the basis of high-resolution gel filtration.

The next question, then, is whether the NOB-modified bovine PLA2 really shows greatly enhanced activity as in the case of porcine PLA2. We did confirm the observation by Tomasselli et al. (1989) that hydrolysis of NOB by porcine PLA2 showed a latency phase. However, the bovine enzyme showed no latency and displayed normal saturation kinetics under the same condition. It was thus possible to determine k_{cat} and K_m values of NOB for WT and K56M, as listed in Table II. The activity of bovine PLA2 toward NOB is comparable to that of K56-acylated porcine PLA2 reported by Tomasselli et al. (1989). Preincubation with NOB did not seem to affect the kinetic behavior and activity of bovine PLA2 toward NOB.

Several conclusions can be reached from these NOB experiments: (i) NOB is a very poor substrate for PLA2 as shown by the data in Table II. Thus, it is questionable whether the acylation by NOB is of any significance to the catalytic

Table II: Summary of Kinetic Data for Monomeric Substrates[a]

enzyme	substrate	k_{cat} (s^{-1})	K_m (mM)	k_{cat}/K_m (M^{-1} s^{-1})
bovine				
WT	DC_7PC	4.5	0.66	6.8×10^3
K56M	DC_7PC	13.5	<0.15	$>90 \times 10^3$
bovine				
WT	DC_6PC	2.4	4.9	0.49×10^3
K56M	DC_6PC	7.7	0.51	15×10^3
K56F	DC_6PC	2.1	1.2	1.8×10^3
K56E	DC_6PC	2.3	4.1	0.56×10^3
bovine				
WT	NOB	0.28	0.18	1.6
K56M	NOB	0.16	0.18	0.9
porcine WT	DC_6PC[b]	0.9	6.0	0.15×10^3
C. adamanteus PLA2	DC_6PC[c]	1.6	4.0	0.40×10^3

[a] The estimated errors for both k_{cat} and K_m are ±15% for PC substrates and ±5% for NOB. [b] From Pieterson (1973). Assays were conducted at pH 6.0 and 25 °C. [c] From Wells (1974).

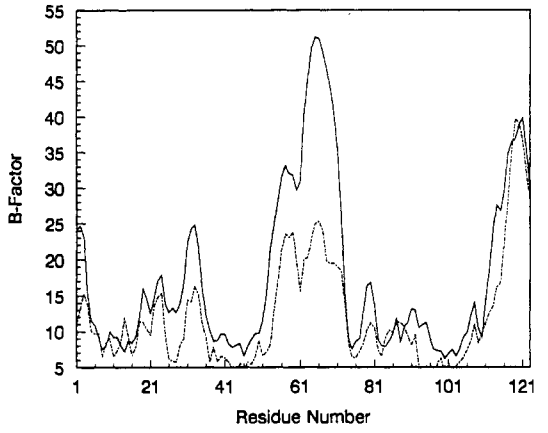

FIGURE 4: Plots of *B*-factors of α-carbons against the residue number for WT (solid lines) and K56M (dashed lines).

mechanism of PLA2. (ii) Acylation does occur for bovine PLA2, but it is not an obligatory step in catalysis. (iii) Some of the important effects of NOB toward *porcine* PLA2 (latency phase and enhanced activity) reported by Tomasselli et al. (1989) were not observed for *bovine* PLA2. Jain et al. (1991a) also failed to observe enhanced activity for the acylated *porcine* PLA2 in scooting mode assays.

Discussion

Possible Structural and Functional Roles of Lys-56. The kinetic results clearly suggest that the side chain of Lys-56 is involved in interacting with substrates. The interaction could occur in three ways in the overall mechanism: interacting with the surface of micelles, interacting with the bound substrate, or both. The former is in agreement with the interfacial site suggested earlier by Dijkstra et al. (1981a). This could also explain why the natural pancreatic PLA2 uses lysine instead of a hydrophobic residue at position 56, since the digestive function of pancreatic PLA2 occurs mainly in the intestine where dietary phospholipids exist in emulsions with bile salts (Waite, 1987), which can be considered negatively charged mixed micelles. In a recent proposal, however, Lys-56 was not included as part of the interfacial site (White et al., 1990; Thunnissen et al., 1990). Although our structural analysis cannot resoluve the role of Lys-56 in the interfacial catalysis, it does clearly suggest that residue 56 is involved in interacting with the bound substrate.

The enhanced activity of K56 mutants could also be a consequence of the structural perturbations in the loop segment that are influenced by the type of side chain at position 56. This relationship between the loop and the activity is supported by three previous observations: (i) Analysis of crystal structures (Renetseder et al., 1985) suggested that one of the main differences between snake venom PLA2 (which have higher activity) and pancreatic PLA2 is that the loop 57–66 is present in pancreatic PLA2 but absent in dimeric snake venom PLA2. (ii) Deletion of this loop from *porcine* pancreatic PLA2 (Δ62–66) also resulted in a 2-fold increase in k_{cat} and a 2-fold decrease in K_m for micellar DC_8PC (Kuipers et al., 1989) as shown in Table I. (iii) In the pro-enzyme (Dijkstra et al., 1982) and the N-terminus-transaminated PLA2 (Dijkstra et al., 1984), both of which show poor activity toward aggregated substrates, the loop was found to be flexible. On the other hand, the loop could just be sensitive to any structural perturbations (Renetseder et al., 1988; Dijkstra et al., 1983) or even crystal packing forces (see Figure 2A), and the perturbations in its conformation may not be related by interfacial catalysis.

Further investigation is required to firmly differentiate these possible interpretations. In addition, whether the other two lysine residues (53 and 57) of the lysine triplet play roles similar to that of Lys-56 remains to be established. Our characterization of the structure–function relationship of the K56 mutants of the bovine pancreatic PLA2, however, has advanced our understanding of the phospholipid head group binding site.

Relationship between K56 Mutants and Acylated PLA2. On the basis of the results of the K56 mutants and that of Tomasselli et al. (1989), one would be tempted to conclude that charge neutralization and/or increased hydrophobicity of the side chain of residue 56 are responsible for the enhanced

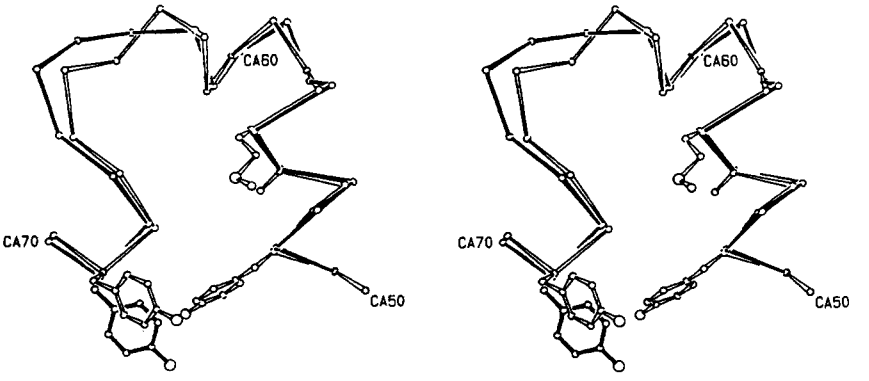

FIGURE 5: Stereoview showing the helix containing the site of mutation and the adjacent loop in WT (solid bonds) and K56M (open bonds). Notice that the backbone of helix and the loop in K56M moved closer compared to WT and that the side chain of Tyr-69 moved substantially. The side chains of the new hydrophobic triplet (Tyr-52, Ala-55, and Met-56) are shown for K56M.

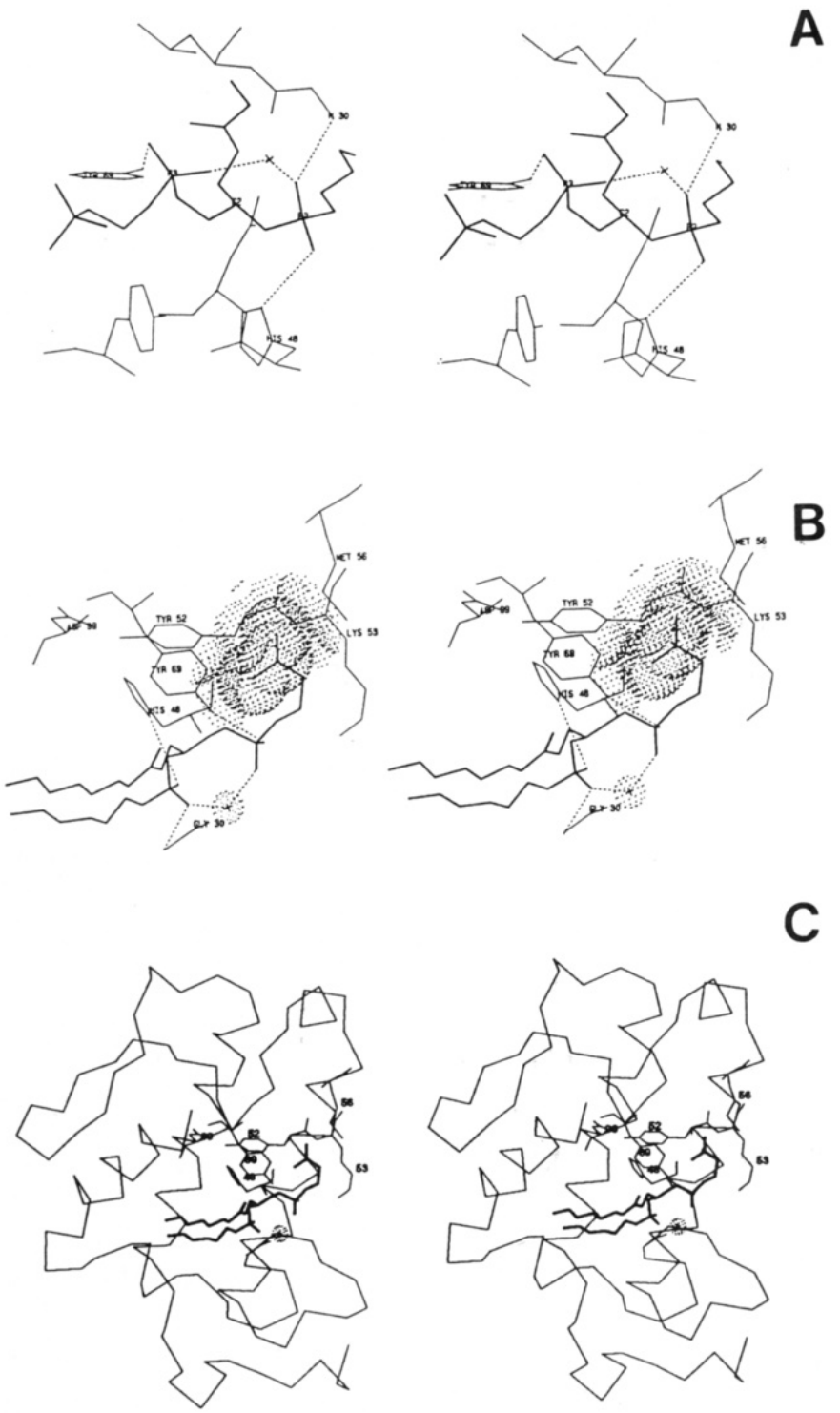

FIGURE 6: Stereoview of the K56M–DC_8PC (tetrahedral analogue) complex obtained by docking the substrate into the enzyme active site according to the interactions indicated by White et al. (1990). The molecular modeling was carried out on an Evans and Sutherland PS330 using FRODO and the geometrical parameters of the substrate were optimized using X-PLOR. Panel A shows the interaction of the inhibitor with the active site residues in a view similar to that of Figure 3 in White et al. (1990). Panel B features the van der Waals interactions (dotted surfaces) between the trimethyl groups of choline and the hydrophobic pocket formed by Met-56, Try-52, and Tyr-69. Panel C shows the α-carbon trace and side chains of a few active site residues of the entire complex. The heavy lines represent the structure of the lipid analogue.

activity in both cases. We do believe that both charge neutralization and hydrophobicity are responsible for the enhanced activities of K56 mutants. The same could be true for the K56-acylated porcine PLA2 even though this is clearly not an obligatory step in catalysis (Jain et al., 1990a). Unfortunately, the assay methods used are different in different groups: the monolayer assay by Tomasselli et al. (1989); the micelle assay in this work; and the vesicle assay by Jain et al. (1991a). These different assays could have different rate-limiting steps. As pointed out by Jain and Berg (1989) and Jain et al. (1991a,b), the monolayer and micelle assays could also be complicated by the E (free enzyme) to E* (enzyme bound to the surface) equilibrium. These complications make it difficult to compare the results from different groups directly. In summary, we have concluded that acylation is not an obligatory step in catalysis, but the detailed kinetic behavior of K56 mutant enzymes (and K56-acylated enzymes) warrants further investigation.

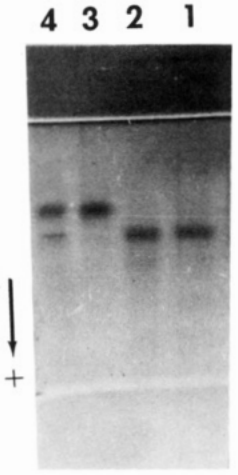

FIGURE 7: Native PAGE analysis of bovine WT PLA2 (lane 3), WT PLA2 treated with NOB (lane 4), K56M (lane 1), and K56M treated with NOB (lane 2). As a control, we have verified that all four samples gave only one band at 14 kDa in the SDS–PAGE gel (not shown).

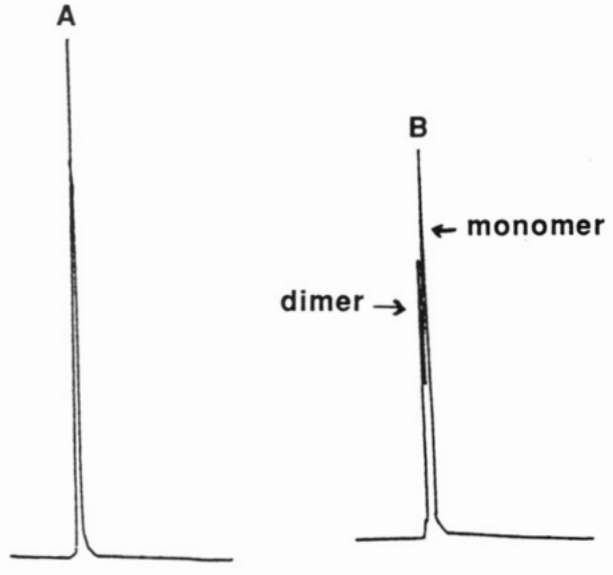

FIGURE 8: Fast flow Sepharose-12 gel filtration chromatography: (A) mixture of WT (monomeric) and K56M bovine PLA2; (B) mixture of *C. atrox* venom PLA2 (dimeric) and K56M bovine PLA2.

ACKNOWLEDGMENTS

We are indebted to Dr. M. K. Jain of the University of Delaware for useful discussions and to Dr. P. Sigler of Yale University for the gift of *Crotalus atrox* PLA2.

REFERENCES

Atkins, G. L., & Nimmo, I. A. (1975) *Biochem. J. 149*, 775–777.

Burley, S. K., & Petsko, G. A. (1985) *Science 229*, 23–28.

Cho, W., Markowitz, M. A., & Kézdy, F. J. (1988) *J. Am. Chem. Soc. 110*, 5166–5171.

de Geus, P., van den Bergh, C. J., Kuipers, O., Verheij, H. M., Hoekstra, W. P. M., & de Haas, G. H. (1987) *Nucleic Acids Res. 15*, 3743–3759.

Deng, T., Noel, J. P., & Tsai, M.-D. (1990) *Gene 93*, 229–234.

Dennis, E. A. (1983) *Enzymes (3rd Ed.) 16*, 307–353.

Dijkstra, B. W., Drenth, J., Kalk, K. H., & Vandermaelen, P. J. (1978) *J. Mol. Biol. 124*, 53–60.

Dijkstra, B. W., Drenth, J., & Kalk, K. H. (1981a) *Nature 289*, 604–606.

Dijkstra, B. W., Kalk, K. H., Hol, W. G. J., & Drenth, J. (1981b) *J. Mol. Biol. 147*, 97–123.

Dijkstra, B. W., van Nes, G. J. H., Kalk, K. H., Brandenburg, N. P., Hol, W. G. J., & Drenth, J. (1982) *Acta Crystallogr., Sect. B 38*, 793–799.

Dijkstra, B. W., Renetseder, R., Kalk, K. H., Hol, W. G. J., & Drenth, J. (1983) *J. Mol. Biol. 168*, 163–179.

Dijkstra, B. W., Kalk, K. H., Drenth, J., de Haas, G. H., Egmond, M. R., & Slotboom, A. J. (1984) *Biochemistry 23*, 2759–2766.

Dupureur, C. M., Deng, T., Kwak, J.-G., Noel, J. P., & Tsai, M.-D. (1990) *J. Am. Chem. Soc. 112*, 7074–7076.

Dutilh, G. E., van Doren, P. J., Verheul, E. A. M., & de Haas, G. H. (1975) *Eur. J. Biochem. 53*, 91–97.

Ghrayeb, J., Kimura, H., Takahara, M., Hsiung, H., Masui, Y., & Inouye, M. (1984) *EMBO J. 3*, 2437–2442.

Jain, M. K., & Berg, O. G. (1989) *Biochim. Biophys. Acta 1002*, 127–156.

Jain, M. K., Ranadive, G., Yu, B.-Z., & Verheij, H. M. (1991a) *Biochemistry 30*, 7330–7340.

Jain, M. K., Rogers, J., Berg, O., & Gelb, M. H. (1991b) *Biochemistry 30*, 7340–7348.

Kuipers, O. P., Thunnissen, M. G. G. M., de Geus, P., Dijkstra, B. W., Drenth, J., Verheij, H. M., & de Haas, G. H. (1989) *Science 244*, 82–85.

Nieuwenhuizen, W., Kunze, H., & de Haas, G. H. (1974) *Methods Enzymol. 32B*, 147–154.

Noel, J. P., & Tsai, M.-D. (1989) *J. Cell. Biochem. 40*, 309–320.

Noel, J. P., Deng, T., Hamilton, K. J., & Tsai, M.-D. (1990) *J. Am. Chem. Soc. 112*, 3704–3706.

Palau, J., & Puigdomenech, P. (1974) *J. Mol. Biol. 88*, 457–469.

Pearson, R. H., & Pascher, I. (1979) *Nature 281*, 499–501.

Pieterson, W. A. (1973) Ph.D. Thesis, University of Utrecht, The Netherlands.

Renetseder, R., Brunie, S., Dijkstra, B. W., Drenth, J., & Sigler, P. B. (1985) *J. Biol. Chem. 260*, 11627–11634.

Renetseder, R., Dijkstra, B. W., Huizinga, K., Kalk, K. H., & Drenth, J. (1988) *J. Mol. Biol. 200*, 181–188.

Rosenberg, A. H., Lade, B. N., Chui, D.-s., Lin. S.-W., Dunn, J. J., & Studier, F. W. (1987) *Gene 56*, 125–135.

Sundaralingam, M. (1972) *Ann. N.Y. Acad. Sci. 195*, 324–355.

Tanaka, T., Kimura, S., & Ota, Y. (1988) *Gene 64*, 257–264.

Taylor, J. W., Schmidt, W., Cosstick, R., Okruszek, A., & Eckstein, F. (1985a) *Nucleic Acids Res. 13*, 8749–8764.

Taylor, J. W., Ott, J., & Eckstein, F. (1985b) *Nucleic Acids Res. 13*, 8765–8785.

Thannhauser, T. W., & Scheraga, H. A. (1985) *Biochemistry 24*, 7681–7688.

Thannhauser, T. W., Konishi, Y., & Scheraga, H. A. (1984) *Anal. Biochem. 138*, 181.

Thunnissen, M. M. G. M., AB, E., Kalk, K. H., Drenth, J., Dijkstra, B. W., Kuipers, O. P., Dijkman, R., de Haas, G. H., & Verheij, H. M. (1990) *Nature 347*, 689–691.

Tomasselli, A. G., Hui, J., Fisher, J., Zürcher-Neely, H., Reardon, I. M., Oriaku, E., Kézdy, F. J., & Heinrikson, R. L. (1989) *J. Biol. Chem. 264*, 10041–10047.

Van den Bergh, C. J., Bekkers, A. C. A. P. A., de Geus, P., Verheij, H. M., & de Haas, G. H. (1987) *Eur. J. Biochem. 170*, 241–246.
Volwerk, J. J., & de Haas, G. H. (1982) *Lipid–Protein Interact. 1*, 69–149.
Waite, M. (1987) *The Phospholipases*, Plenum Press, New York.
Wells, M. A. (1974) *Biochemistry 13*, 2248–2257.
White, S. P., Scott, D. L., Otwinowski, Z., Gelb, M. H., & Sigler, P. (1990) *Science 250*, 1560–1563.

Aggregation of IGF-I Receptors or Insulin Receptors and Activation of Their Kinase Activity Are Simultaneously Caused by the Presence of Polycations or K-ras Basic Peptides†

Qin-Yu Xu, Shu-Lian Li, Thomas R. LeBon, and Yoko Fujita-Yamaguchi*
Department of Molecular Genetics, Beckman Research Institute of the City of Hope, 1450 East Duarte Road, Duarte, California 91010

Received March 18, 1991; Revised Manuscript Received September 13, 1991

ABSTRACT: Several groups including us reported that basic proteins and polycations activate the insulin receptor tyrosine-specific protein kinase (TPK) in vitro. However, some inconsistency has become obvious in the observations. The most intriguing was the brief description by Morrison et al. [(1989) *J. Biol. Chem. 264*, 9994–10001] that polylysine had no effect on the IGF-I receptor TPK despite its 84% identity to the insulin receptor TPK. In the present study, we used highly purified IGF-I and insulin receptor TPKs in an effort to solve the discrepancies noted in the recent publications and to reveal the mechanism by which polycations stimulate the receptor TPKs. We report that the IGF-I receptor TPK is stimulated by polycations and basic proteins in a manner similar to their effects on the insulin receptor TPK. When effects of polylysine and polyarginine on both receptor TPKs were closely compared, subtle qualitative differences were found: Polylysine stimulated autophosphorylation and exogenous substrate phosphorylation activities of both insulin receptor TPK and IGF-I receptor TPK similarly. In contrast, another polycation, polyarginine, affected both TPKs in a manner quite different from polylysine: Polyarginine stimulated insulin receptor autophosphorylation to a greater extent than polylysine did while it had a very small effect on the IGF-I receptor autophosphorylation as well as the exogenous substrate phosphorylation activities of the two receptor TPKs. We have further extended the studies to include the domains of natural proteins which contain a polylysine-like sequence. Such peptides, K-ras peptides, had similar effects on the two receptor TPKs to those of polycations. Finally, we observed that polycations and K-ras peptides caused receptor aggregation as judged by nondenaturing gradient polyacrylamide gel electrophoresis and sucrose density gradient centrifugation. These studies suggest a strong correlation between receptor aggregation and activation of IGF-I and insulin receptor TPKs which may be caused by cellular proteins such as K-ras products.

Insulin-like growth factor I (IGF-I)[1] and insulin receptors are membrane-bound glycoproteins that are composed of two extracellular α subunits and two transmembrane β subunits. The β subunit carries cytoplasmic tyrosine-specific protein kinase (TPK) activity. Ligand binding to the receptor extracellular domain induces autophosphorylation of the β subunit and activation of the TPK. This TPK activation process is required for some or all of IGF-I's and insulin's transmembrane signaling (Rosen, 1987; Goldfine, 1987; Roth et al., 1988; Czech, 1989). Hence, further characterization of the TPKs is essential to understand the signal transduction mechanisms of IGF-I and insulin.

We and others recently reported that basic proteins and polycations activate the insulin receptor TPK in vitro (Fujita-Yamaguchi et al., 1989a; Sacks et al., 1989a; Sacks & McDonald, 1988; Rosen & Lebwohl, 1988; Morrison et al., 1989; Kohanski, 1989). Sacks et al. first observed that protamine and polylysine activate phosphorylation of the β subunit (Sacks et al., 1989a; Sacks & McDonald, 1988). Rosen and Lebwohl postulated that polylysine alters divalent cation requirements of the insulin receptor TPK (Rosen & Lebwohl, 1988) whereas we suggested that polylysine directly interacts with the β subunit, thereby activating the receptor TPK independently of insulin (Fujita-Yamaguchi et al., 1989a). Morrison et al. characterized effects of polylysine and divalent metals on insulin and IGF-I receptor TPKs (Morrison et al., 1989). In contrast to our results, they observed that polylysine activates insulin receptor TPK only in the presence of insulin. In addition, they found that polylysine was completely unable to stimulate IGF-I receptor TPK. In light of the structural homology between the two TPKs, 84% identity at the amino acid sequence level (Ullrich et al., 1986), this striking difference in the polylysine effect on the two TPKs reported by Morrison et al. (1989) required further verification. Finally, Kohanski reported that both polylysine and polyarginine

† This work was supported by Grant DK34427 from the National Institutes of Health.
* To whom correspondence should be addressed.

[1] Abbreviations: TPK, tyrosine-specific protein kinase; IGF-I, insulin-like growth factor I; SDS, sodium dodecyl sulfate; PAGE, polyacrylamide gel electrophoresis; Tris-HCl, tris(hydroxymethyl)aminomethane hydrochloride.

0006-2960/91/0430-11811$02.50/0